The zebrafish operculum: a powerful system to assess osteogenic bioactivities of molecules with pharmacological and toxicological relevance

Marco Tarasco, Vincent Laizé, João Cardeira, M. Leonor Cancela, Paulo J. Gavaia

PII: S1532-0456(17)30091-1
DOI: doi:10.1016/j.cbpc.2017.04.006
Reference: CBC 8316

To appear in: *Comparative Biochemistry and Physiology Part C*

Received date: 14 March 2017
Revised date: 20 April 2017
Accepted date: 25 April 2017

Please cite this article as: Tarasco, Marco, Laizé, Vincent, Cardeira, João, Leonor Cancela, M., Gavaia, Paulo J., The zebrafish operculum: a powerful system to assess osteogenic bioactivities of molecules with pharmacological and toxicological relevance, *Comparative Biochemistry and Physiology Part C* (2017), doi:10.1016/j.cbpc.2017.04.006

The zebrafish operculum: a powerful system to assess osteogenic bioactivities of molecules with pharmacological and toxicological relevance

Marco Tarasco[1], Vincent Laizé[1], João Cardeira[1,2], M. Leonor Cancela[1,3], Paulo J. Gavaia[1,3,*]

[1] Centre of Marine Sciences (CCMAR), [2] ProRegeM PhD Programme, Department of Biomedical Sciences and Medicine, University of Algarve, Campus de Gambelas, Faro, Portugal, [3] Department of Biomedical Sciences and Medicine, University of Algarve, Campus de Gambelas, Faro, Portugal

ms. has 31 pages, 6 figures, 4 suppl. files

* Corresponding author:
Paulo J. Gavaia, PhD
CCMAR / University of Algarve, Campus de Gambelas, 8005-139 Faro, Portugal
Phone: +351.289.800057, +351.289.800900 ext. 7217
Fax: +351.289.800 069
email: pgavaia@ualg.pt

Abstract

Bone disorders affect millions of people worldwide and available therapeutics have a limited efficacy, often presenting undesirable side effects. As such, there is a need for novel molecules with bone anabolic properties. The aim of this work was to establish a rapid, reliable and reproducible method to screen for molecules with osteogenic activities, using the zebrafish operculum to assess bone formation. Exposure parameters were optimized through morphological analysis of the developing operculum of larvae exposed to calcitriol, a molecule with known pro-osteogenic properties. An exposure of 3 days initiated at 3 days post-fertilization was sufficient to stimulate operculum formation, while not affecting survival or development of the larvae. Dose-dependent pro- and anti-osteogenic effects of calcitriol and cobalt chloride, respectively, demonstrated the sensitivity of the method and the suitability of the operculum system. A double transgenic reporter line expressing fluorescent markers for early and mature osteoblasts was used to gain insights into the effects of

calcitriol and cobalt at the cellular level, with osteoblast maturation shown to be stimulated and inhibited, respectively, in the operculum of exposed fish. The zebrafish operculum represents a consistent, robust and rapid screening system for the discovery of novel molecules with osteogenic, anti-osteoporotic or osteotoxic activity.

Keywords

Zebrafish; Operculum; Screening; Osteogenesis; Calcitriol

Introduction

Osteoporosis and osteopenia are common bone diseases affecting millions of people worldwide (Pisani et al., 2013) and are characterized by both reduced mass and the structural deterioration of bone, causing its fragility and increased susceptibility to fractures. Several drugs are currently available to prevent or limit deleterious effects of osteoporosis and osteopenia, e.g. vitamin D supplements (Feng and McDonald, 2011), bisphosphonates (McClung et al., 2013), antibodies (Miller, 2009), and RANKL inhibitors (Bernabei, 2014), but they have only a limited efficacy and often present undesirable side effects (Bernabei, 2014). As such, there is a need for novel molecules with bone anabolic properties that could successfully counter low bone mass, while having limited or no side effects.

Currently, the screening methods, rather than molecule availability, represent a bottleneck toward the discovery of pro-osteogenic compounds. Robustness, high-throughput and simplicity are critical features of a good screening method. While *in vitro* cell systems are often used as pre-screenings to reduce animal experimentation, *in vivo* animal systems are preferred as they provide the physiological conditions for an integrated response to compound exposure. In the last decade, the zebrafish *Danio rerio* (Hamilton, 1822) has been successfully used in biomedical and pharmaceutical research to model several human disorders (Laizé et al., 2014) and screen (MacRae and Peterson, 2015) for compounds with the ability to rescue or prevent these disorders.

Success of the zebrafish lies in the many technical advantages over classical model animals (e.g. rodents), allowing quick, inexpensive, large-scale and high-throughput screening for new molecules with pharmacological effects (Lieschke and Currie, 2007). Of critical importance for large-scale screening, or when limited amounts of compounds are available, is the use of small size larvae, which can be easily

accommodated in 96-well plates, with each well filled with as little as 200 µL of test solution. Waterborne exposure of the zebrafish to the molecules also represents a reliable and simple way of drug delivery (Wilkinson and Pritchard, 2014). Furthermore, any osteogenic effect is easily detected since the body at these developmental stages is translucent and allow the visualization of mineralized tissues after proper staining (Walker and Kimmel, 2007). Other features, such as robustness, high fecundity and short generation time have reinforced the suitability of zebrafish as a laboratory animal. Various *in vivo* tools exist to study how drugs affect the skeleton (osteogenic or anti-osteogenic activities) (Laizé et al., 2014; Cardeira et al., 2016), including zebrafish mutant lines mimicking human skeletal disorders (Barrett et al., 2006; de Vrieze et al., 2014) and transgenic lines able to express fluorescent markers at sites of bone-related gene expression (Knopf et al., 2011a). These are valuable, both for the discovery of therapeutic molecules capable of rescuing skeletal pathologies and in studying their mechanisms of action.

The first skeletal structures to develop and ossify, such as the cleithrum, pharyngeal teeth, basioccipital articulatory process and supra mandibular, can be detected as soon as 3-4 days post fertilization (dpf) (Gavaia et al., 2006). The operculum is among the first dermal bones to ossify and can be positively stained by alizarin red S (AR-S) at 3 dpf, i.e. shortly after hatching (Kimmel et al., 2010). The operculum, being flat in shape and localized at the surface of the fish head, can also be easily imaged and assessed morphometrically. Additionally, previous studies have shown that it can be used to evaluate bone morphogenetic variations (Huycke et al., 2012). Therefore, it represents a bone of choice to screen the effects of osteogenic compounds in zebrafish larvae.

This study aims to establish and optimize a methodology to easily screen for potential bioactives in laboratories using zebrafish. This novel method should overcome limitations of current systems used to assess osteogenic effects in zebrafish, such as long exposure time, late assessment, no correction for inter-specimen variability, but also long image acquisition and analysis. The development of the zebrafish operculum will be followed during larval development and several parameters evaluated to reduce inter-specimen variability. Calcitriol (1α,25-dihydroxyvitamin D_3), a well-known osteogenic compound (Fleming et al., 2005), will be used to establish optimal conditions of exposure and evaluate dose response in zebrafish larvae. Cobalt chloride, a known osteotoxicant, will be tested to assess the capacity of

the operculum to also evaluate compounds with anti-osteogenic activity. Finally, the suitability of a double transgenic line, expressing fluorescence proteins under the control of bone marker gene promoters, will be tested to gain insights into the mechanisms underlying the osteogenic effects of calcitriol and cobalt.

Materials and methods

Ethics statement on animal experiments

All the experimental procedures involving animals followed the EU Directive 2010/63/EU and National Decreto-Lei 113/2013 legislation for animal experimentation and welfare. Animal handling and experiments were performed by qualified operators accredited by the Portuguese Direção-Geral de Alimentação e Veterinária (DGAV).

Zebrafish egg production

Sexually mature zebrafish (AB wild-type strain or transgenic lines *Tg(Ola.sp7:mCherry)* (Singh et al., 2012) and *Tg(Ola.osteocalcin:EGFP)* (Knopf et al., 2011b) abbreviated thereafter as *sp7:mCherry* and *oc:EGFP*) were crossed using an in-house breeding program. Fertilized eggs were transferred into a 1-L container with static water conditions and the following parameters: temperature 28 ± 0.1 °C, pH 7.5 ± 0.1, conductivity 700 ± 50 μS, NH_3 and NO_2 lower than 0.1 mg/L, NO_3 at 5 mg/L and a photoperiod of 14-10 h light-dark. Fish water was prepared by adding a salt mixture (Instant Ocean, Blacksburg, VA) and sodium bicarbonate to reverse osmosis treated water in order to maintain stable pH and conductivity. Methylene blue (0.0002% w/v) was added to prevent fungal growth. At 5 days post-fertilization (dpf), water was renewed and larvae fed with *Artemia* (5 nauplii per mL; strain AF from INVE Aquaculture, Dendermonde, Belgium) every day.

Exposure to calcitriol and cobalt chloride

At appropriate times, larvae were transferred to 6 well-plates when using AB larvae (15 larvae in 10 mL of water) or to plastic cups when using double transgenic *Tg(sp7:mCherry/oc:EGFP)* larvae (100 larvae in 70 mL of water). Individuals were exposed to different concentrations of either calcitriol (Sigma-Aldrich, St. Louis, MO) (1, 3.16, 10 and 31.6 pg/mL), cobalt chloride ($CoCl_2$; Sigma-Aldrich) (0.04, 0.126, 0.4, 1.26, and 4 mg/L) and their respective solvent i.e. 0.1% ethanol (Merck,

Darmstadt, Germany) for calcitriol and H_2O for cobalt chloride. Treatment medium was renewed (70% of the total volume) daily until the end of the treatment period. At that time, larvae were sacrificed with a lethal dose of MS-222 (0.6 mM, pH 7.0, Sigma-Aldrich), stained for 15 min at room temperature with 0.01 % alizarin red S (AR-S) prepared in Milli-Q water (pH 7.4), and washed twice with Milli-Q water for 5 min (method adapted from Bensimon-Brito et al. (2016)). Larvae were imaged immediately after euthanasia.

Tartrate-resistant acid phosphatase staining

Wild-type zebrafish larvae (AB) were sampled every 24 h from 6 to 20 dpf, dehydrated through an ice-cold increasing ethanol series and preserved at -20 °C. Before tartrate-resistant acid phosphatase (TRAP) staining, specimens were rehydrated, washed with PBS and incubated at room temperature in a 0.1 M sodium acetate buffer (pH 5.1, Sigma-Aldrich) containing 50 mM of L-(+)-tartaric acid (Sigma-Aldrich). Larvae were incubated in the dark and TRAP activity was revealed using naphthol AS-TR phosphate as substrate and hexazotized pararosaniline, as previously described by Witten (1997). Larvae previously heated at 90 °C for 5 min before staining, or incubated without substrate, were used as negative control. Larvae were preserved in 75% glycerol (Biochem Chemopharma, Cosne sur loire, France) until image acquisition.

Image acquisition and morphometric analysis

Euthanized larvae were placed in a lateral plane on top of a 2% agarose gel. AB larvae stained with alizarin red S were imaged using a MZ 7.5 fluorescence stereomicroscope (Leica, Wetzlar, Germany) equipped with a green light filter (λ_{ex} = 530-560 nm and λ_{em} = 580 nm) and a black-and-white F-View II camera (Olympus, Hamburg, Germany). Images were acquired using the following parameters: exposure time 1 s, gamma 1.00, image format 1376×1032 pixels, binning 1×1. Fluorescence images were analyzed using ImageJ 1.49v software. For morphometric analysis, color channels of the RGB images were split. Red channel (8-bit) images were used for further analyses. Brightness and contrast were optimized to enhance the visibility of cranial bones, in particular the operculum. The minimum and maximum displayed pixel values were set to 0 and 69 respectively. The area of the head and operculum, the length between the snout to the cleithrum, and the width and height of the eye and

iris, were determined using built-in tools. The areas of the eye and iris were calculated using the ellipse area formula (½ width × ½ height × π). Transgenic larvae *Tg(sp7:mCherry/ oc:EGFP)* were imaged using a SteREO Lumar.V12 fluorescence stereomicroscope (Zeiss, Oberkochen, Germany) equipped with GFP (λ_{ex} = 470-440 nm; λ_{em} = 525-550 nm) and TxRed (λ_{ex} = 565-530 nm; λ_{em} = 620-660 nm) filters and an AxioCam MR3 camera (Zeiss). Images were acquired according to the following parameters: 16-bit black-and-white image, exposure time 120 ms (bright field) or 1 s (fluorescence), gamma 1.00, image format 692×520 pixel, binning 2×2 and 20 Z-stacks (fluorescence). For both red and green channels, Z-stacks were merged and aligned through the extended focus built-in tool of the AxioVision software. Fluorescence images (red and green channels) were 8-bit transformed in ImageJ and both the number of fluorescent pixels (pixel values above threshold values) and the areas of fluorescence were determined for each operculum using built-in tools (see example in Figure 5A and detailed protocol in Supplementary Table 1). The area of the head was determined from bright-field images.

Bright-field images of TRAP-stained AB larvae were acquired using a SteREO Lumar.V12 stereomicroscope and the following parameters: 16-bit RGB image, exposure time 100 ms, gamma 1.00, image format 1384×1040 pixel, binning 1x1.

Statistical analysis

Statistical differences were determined through one-way ANOVA followed by Dunnett's multiple comparison test (p<0.05) or through unpaired t-tests with Welch's correction (p<0.05). The correlation between selected morphometric parameters was evaluated through a simple linear regression and the R-squared value. Statistical analyses were performed using Prism version 6.00 (GraphPad Software, Inc. La Jolla, CA).

Results

Time course of operculum formation

Wild type zebrafish larvae (AB) were sampled every 24 h from 4 to 15 dpf and stained with alizarin red S to reveal mineralized bone structures, in particular the operculum. Fluorescence images of the lateral view of the head of each larva were acquired (Figure 1A) and the morphometry of the different elements and structures

was analyzed (Figure 1B). The area of the head (A1) and operculum (A2), the length from the snout to the cleithrum (L1), the width and height of both eye and iris (L2/L3 and L4/L5, respectively) were determined. Subsequently, the suitability of the different measurements to correct for inter-specimen variability in operculum area was assessed through simple linear regressions and averaged coefficient of variance (CV). While both the area of the iris and the eye and the length between snout and cleithrum exhibited a good correlation with the area of the operculum (R^2 = 0.88, 0.90 and 0.92, respectively), the area of the head appeared to be the most accurate parameter to correct for inter-specimen variability of the operculum area (R^2 = 0.94), which also showed the lowest CV (27.0 ± 9.9 %) (Supplementary figure 1). Monitored from 4 to 15 dpf (Figure 2A), the operculum area was plotted as a function of time, either as raw data (Figure 2B) or after correction by the area of the head (operculum area divided by the head area, O/H) (Figure 2C), and CV was estimated. Averaged CV for all time points was markedly reduced upon correction for head size (51.9 ± 25.2 % *versus* 27.0 ± 9.9 %), indicating that variation in operculum area due to inter-specimen variability in sampled populations could be efficiently corrected. Analysis of corrected operculum area during zebrafish development revealed different growth phases, 4-6 dpf being the phase with the highest growth rate (208%).

Effect of calcitriol on zebrafish operculum mineralization

The effect of calcitriol (10 pg/mL) on operculum formation was assessed using the above-described methodology. Larvae were exposed to calcitriol for different periods (3, 6 and 9 days) and exposure was initiated at different developmental stages (3, 5 and 8 dpf) (Figure 3). It is important to mention that calcitriol did not affect the area of the head, the parameter used to correct operculum area (Supplementary Figure 2). 3 day long exposure to calcitriol stimulated operculum formation/mineralization when initiated at 3 or 5 dpf, with an increase of 41.80 ± 7.83 % and 36.46 ± 6.37 %, respectively (Figures 3A, 3B). However, when the exposure started at 8 dpf no significant effects were observed in operculum size (Figure 3C). A longer exposure to calcitriol (6 days) also increased operculum area when initiated at 3 and 5 dpf, with an increase of 58.42 ± 23.73 % and 74.37 ± 21.68 %, respectively (Figures 3D, 3E), while onset at 8 dpf did not significantly affect operculum size (Figure 3F) and strongly affected survival. Operculum area was also increased upon exposure to calcitriol for 9 days (Figures 3G, 3H), but this increase was only statistically

significant when exposure was initiated at 3 dpf (90.56 ± 30.59 %). Generally, fish survival (indicated in Figure 3) was affected by exposure longer than 3 days and exposure initiated after 5 dpf, supporting the suitability of a short and early exposure of the larvae.

Osteogenic effect on the operculum is concentration-dependent

Operculum formation was then assessed in fish exposed to several concentrations of calcitriol and cobalt chloride. While exposure to 1 pg/mL of calcitriol slightly increased operculum formation (10.45 ± 6.21 %, not statistically different from control), exposure to higher concentrations – 3.16, 10 and 31.6 pg/mL – resulted in a dose-dependent increase of the operculum area (27.92 ± 6.21 %, 34.98 ± 4.79 % and 43.52 ± 6.76 %, respectively; Figure 4). Exposure to cobalt chloride – 0.4, 1.26 and 4 mg/L – caused a decrease in operculum formation, also in a dose-dependent manner (11.65 ± 3.72 %, 26.57 ± 3.82% and 68.40 ± 5.85%, respectively; Figure 4), while the area of the head was not affected (data not shown). However, the exposure of zebrafish larvae to 4 mg/L of cobalt chloride affected their survival. Results collected from fish exposed to calcitriol and cobalt chloride indicated that the zebrafish operculum system is suitable to study the dose-dependent effect of pro- and anti-osteogenic molecules.

Calcitriol and cobalt exposure alter osteoblast maturation

Zebrafish transgenic lines expressing green and red fluorescent proteins under the control of the promoters of two osteoblast markers – *osterix* (*sp7*), a marker of early osteoblasts and *osteocalcin* (*oc*), a marker of mature osteoblasts – were used to gain insights into cellular dynamics underlying the osteogenic effects observed during operculum formation. Double transgenic larvae *Tg(sp7:mCherry/oc:EGFP)* at 3 dpf were exposed for 3 days to calcitriol or cobalt chloride, and the effects on osteoblasts were assessed through the analysis of fluorescence images at 6 dpf (Figure 5B). Exposure to calcitriol (10 pg/mL) increased the operculum area positive for *sp7:mCherry* by 32.28 ± 6.76 % (Figure 5C), suggesting that early osteoblast population was probably increased due to an increment of cell proliferation. Exposure to calcitriol also increased the operculum area positive for *oc:EGFP* (Figure 5C), although a stronger effect was observed (83.61 ± 10.69 %), indicating that cell differentiation/mature osteoblast population may be stimulated with calcitriol

treatment. An analysis of the number of fluorescent pixels per operculum area further confirmed the specific effect of calcitriol on late osteoblast populations (515.20 ± 164.50 % increase in calcitriol-treated fish; Figure 5D), while the effect on early osteoblast populations was mild (36.43 ± 13.34 % increase in calcitriol-treated fish; Figure 5D). Exposure to cobalt chloride (4 mg/L) decreased the operculum area positive for *oc:EGFP* (68.00 ± 11.24 %), an effect confirmed by pixel analysis (94.11 ± 21.74 %; Figure 5D), which would suggest the inhibition of osteoblast maturation upon exposure to cobalt chloride. No effect was observed on early osteoblast population. The absence of TRAP activity in the operculum of larvae younger than 13 dpf (Supplementary figure 3) and in larvae exposed to cobalt from 3 to 6 dpf (results not shown) suggested that osteoclasts do not play a role in the anti-osteogenic effect of cobalt chloride.

Discussion

The purpose of this work was to establish a simple, reproducible and reliable zebrafish-based screening method to assess the osteogenic effects of extracts or molecules. Because it is a surface bone that forms early during development and can therefore be easily monitored in larval stages, the operculum represents a skeletal structure with a high potential for molecule screening assays. The suitability of zebrafish alizarin red S-stained operculum to screen for osteogenic compounds was established, and the duration and initiation times of larval exposure optimized.

Analysis of the complete data set revealed that although the osteogenic effects of calcitriol were detected in most of the conditions, a short (3 day) and early (3 dpf) exposure – a situation favoured in fast screening methods – was proven more appropriate and reliable. In these economically favourable conditions (i.e. short exposure time and early treatment synonymous with a limited use of compound and high animal turnover), the operculum exhibited the highest growth increment (208 %), while the mortality associated with the housing conditions (e.g. limited space as larvae grow and degraded water quality due to static conditions) was minimal. Increased mortality observed over longer exposures or with older larvae has been principally associated with housing conditions. However, it may also be related to the point-of-no-return (PNR), when zebrafish larvae, after switching from endogenous nutritional reserves to exogenous feeding (5-7 dpf), are not able to feed and do not recover even if food becomes available (Gerking, 2014). PNR is associated

with increased mortality and screening should therefore end before this point, both to minimize stress and avoid mortality not related to the test conditions with molecules or extracts. Accordingly, we propose that the screening or study of osteogenic bioactivities in zebrafish larvae should be initiated at 3 dpf and last for 3 days (Figure 6). Although this should be further tested (e.g. using a panel of hundreds of compounds or small molecule libraries), the optimized operculum system described here, may provide a throughput higher than existing methodologies currently available to assess osteogenic compounds/activities.

An approach using alizarin red S staining combined with morphometric analysis has already been demonstrated as an easy and accurate way to detect and quantify bone mineral deposition under fluorescence conditions (Bensimon-Brito et al., 2016; Cardeira et al., 2016). Other techniques – e.g. X-rays or micro-computed tomography – have been used to image mineralized structures in zebrafish, but their application in the context of the methodology presented here may be difficult due to technical limitations; long acquisition time (micro-CT) or low image resolution of poorly mineralized larvae (X-ray) (Bruneel and Witten, 2015; Hosen et al., 2013).

This study also considered the necessity to correct for inter-specimen variability and, while several parameters were deemed appropriate, the area of the head proved most precise in calibrating operculum area measurements; while also being easily determined from the same set of images used to assess operculum area. Several studies have reported the use of alizarin red S to screen for molecules with osteogenic and mineralogenic bioactivities in zebrafish. They assessed the mineralization of cranial bones in larvae exposed from 3 to 9 dpf (Luo et al., 2016), or the count of vertebral bodies at 10 dpf (Yu et al., 2008), but none considered inter-specimen variability or accurately quantified the osteogenic effect. They also failed to provide a medium/high-throughput approach, utilised long exposures, late endpoints and a laborious image acquisition procedure, and therefore have limited applicability for large-scale screening of molecules.

Calcitriol, the bioactive form of vitamin D, was used throughout this study to optimize the screening procedure, but also to validate the mineralizing operculum as a suitable system to monitor osteogenic bioactivities. Calcitriol is a well-known osteogenic and anti-osteoporotic compound (Bernabei, 2014) that stimulates osteoblastic growth and differentiation, and therefore bone formation *in vivo* (Liu et al., 2015) and mineralization *in vitro* (Woeckel et al., 2010). Calcitriol also increases

bone formation in zebrafish skeletal structures, such as in the perichordal sheath and coracoid processes, after exposure from 3 to 9 dpf (at concentrations higher than 25 fg/mL) (Fleming et al., 2005) and in maxilla, branchiostegal rays, hyomandibulars, entopterygoids and ceratohyal after exposure from 5 to 10 dpf (at 200 ng/mL) (Aceto et al., 2015).

A pro-osteogenic effect of calcitriol on zebrafish opercular development is reported here for the first time. The anabolic effect of calcitriol on zebrafish bone was found to be dose-dependent, demonstrating the sensitivity of the operculum system and therefore its suitability to screen for osteogenic compounds. The dose-dependent reduction of the operculum area observed upon exposure to cobalt chloride, a metal already shown to negatively affect osteoblast differentiation *in vitro* (Osathanon et al., 2014) and to promote bone resorption (Patntirapong et al., 2009), further indicated the capacity of the operculum system to assess anti-osteogenic compounds. It may therefore have potential application in the field of ecotoxicology, e.g. to identify osteotoxic chemicals.

This study also aimed at testing the suitability of transgenic zebrafish lines to gain insights into the mechanisms underlying osteogenic effects observed in wild-type larvae stained with alizarin red S. Among the several transgenic zebrafish lines available to study bone formation and skeletogenesis (Hammond and Moro, 2012), *Tg(sp7:mCherry/oc:EGFP)* has already been successfully used to assess the role of early/late osteoblasts during *de novo* bone formation throughout zebrafish development (Bensimon-Brito et al., 2012) and caudal fin regeneration (Singh et al., 2012). The positive effect of calcitriol on osteoblast maturation in the developing operculum of zebrafish larvae is reported here for the first time using this transgenic line. We propose that increased osteoblastogenesis – not reduced osteoclastogenesis – is probably the primary mechanism in the promotion of operculum growth and mineralization in larvae aged 3-6 dpf. A mechanism involving reduced osteoclast activity was ruled out since the onset of TRAP activity in the operculum was detected in larvae aged 13 dpf, an event confirmed by previous reports (Hammond and Schulte-Merker, 2009; Witten et al., 2001). A stimulation of osteocalcin transcription by osteoblasts upon exposure to calcitriol has already been reported *in vitro* in human and murine cell systems and *in vivo* in transgenic mice, and has been associated with the presence of binding elements for a vitamin D receptor within the promoter of the osteocalcin gene (Nakanishi et al., 2013; Thomas et al., 2000).

Osteocalcin is a bone matrix protein mainly produced by mature osteoblasts (Capulli et al., 2014), that is involved in calcium (Hoang et al., 2003) binding and consequently in bone matrix formation and mineralization, being recognized as a regulator of hydroxyapatite crystal deposition and maturation (Gavaia et al., 2006; Razzaque, 2011). The stimulation of osteocalcin transcription by calcitriol is probably a critical step in the osteogenic effect on zebrafish operculum, as demonstrated by data collected from the osteocalcin transgenic line. Similarly, we propose that decreased osteoblastic maturation – not increased osteoclastogenesis – is probably the primary mechanism in the reduced operculum growth in larvae exposed to cobalt chloride between 3-6 dpf, an hypothesis supported by the inhibition of osteocalcin transcription observed in cobalt-exposed osteoblast-like cells (Osathanon et al., 2014). Although the analysis of the fluorescent area and pixel number provided comparable results (i.e. a stimulation or inhibition of osteocalcin-related signal), we believe that area measurements are more appropriate. They allow faster data acquisition, while analysis of pixel number is more time consuming but ultimately delivers more trustworthy data.

In conclusion, we have established the suitability of the zebrafish operculum to screen for molecules with osteogenic activity. Furthermore, we have developed a methodology allowing for an accurate and rapid assessment of changes in operculum formation and mineralization, that can be applied to medium/large scale screening of molecules. Dose-dependent effects of both calcitriol and cobalt chloride confirmed the sensitivity of this system and its applicability to the study of compounds with pro/anti-osteogenic activity. The use of transgenic zebrafish lines, for osteoblast-specific marker genes, has proven valuable for gaining insight into the cellular mechanism associated with the observed osteogenic effects. The implementation of alizarin red S as a vital stain in zebrafish (Bensimon-Brito et al., 2016; Cardeira et al., 2016) could represent a future improvement of the method presented here. This would reduce animal experimentation and therefore further strengthen the suitability of zebrafish to study bone development, complementing traditional mammalian models.

Acknowledgements

João Cardeira acknowledges the financial support from the Portuguese Foundation for Science and Technology (FCT) through the doctoral grant PD/BD/52425/2013 of the ProRegeM PhD Programme (PD/00117/2012). This work was funded in part by the

FCT and the European Commission (ERDF-COMPETE) through PEst-C/MAR/LA0015/2011 project and by the FCT through UID/Multi/04326/2013 and PTDC/MAR/112992/2009 (AQUATOX) projects. The help of Gil Martins (zebrafish breeding), Matthew Carson (manuscript proofreading) and Claudia Florindo (Light Microscopy Facility of CBMR/UAlg) is gratefully acknowledged.

References

Aceto, J., Nourizadeh-Lillabadi, R., Marée, R., Dardenne, N., Jeanray, N., Wehenkel, L., Aleström, P., van Loon, J.J.W.A., Muller, M., 2015. Zebrafish Bone and General Physiology Are Differently Affected by Hormones or Changes in Gravity. PLoS One 10, e0126928. doi:10.1371/journal.pone.0126928

Barrett, R., Chappell, C., Quick, M., Fleming, A., 2006. A rapid, high content, in vivo model of glucocorticoid-induced osteoporosis. Biotechnol. J. 1, 651–655.

Bensimon-Brito, A., Cardeira, J., Cancela, L., Huysseune, A., Witten, E., 2012. Distinct patterns of notochord mineralization in zebrafish coincide with the localization of Osteocalcin isoform 1 during early vertebral centra formation.

Bensimon-Brito, A., Cardeira, J., Dionísio, G., Huysseune, A., Cancela, M.L., Witten, P.E., 2016. Revisiting in vivo staining with alizarin red S - a valuable approach to analyse zebrafish skeletal mineralization during development and regeneration. BMC Dev. Biol. 16, 2.

Bernabei, R., 2014. Screening , diagnosis and treatment of osteoporosis : a brief review. Clin. Cases Miner. Bone Metab. 11, 201–207.

Bruneel, B., Witten, P.E., 2015. Power and challenges of using zebrafish as a model for skeletal tissue imaging. Connect. Tissue Res. 56, 161–173.

Capulli, M., Paone, R., Rucci, N., 2014. Osteoblast and osteocyte: Games without frontiers. Arch. Biochem. Biophys. 561, 3–12. doi:10.1016/j.abb.2014.05.003

Cardeira, J., Gavaia, P.J., Fernández, I., Cengiz, I.F., Moreira-Silva, J., Oliveira, J., Reis, R., Cancela, M.L., Laizé, V., 2016. Quantitative assessment of the regenerative and mineralogenic performances of the zebrafish caudal fin. Sci. Rep. 6, 39191.

de Vrieze, E., van Kessel, M.A., Peters, H.M., Spanings, F.A.T., Flik, G., Metz, J.R., 2014. Prednisolone induces osteoporosis-like phenotype in regenerating zebrafish scales. Osteoporos. Int. 25, 567–578.

Feng, X., McDonald, J.M., 2011. Disorders of Bone Remodeling. Annu. Rev. Pathol.

Mech. Dis. 6, 121–145.

Fleming, A., Sato, M., Goldsmith, P., 2005. High-throughput in vivo screening for bone anabolic compounds with zebrafish. J. Biomol. Screen. 10, 823–831.

Gavaia, P.J., Simes, D.C., Ortiz-Delgado, J.B., Viegas, C.S.B., Pinto, J.P., Kelsh, R.N., Sarasquete, M.C., Cancela, M.L., 2006. Osteocalcin and matrix Gla protein in zebrafish (Danio rerio) and Senegal sole (Solea senegalensis): Comparative gene and protein expression during larval development through adulthood. Gene Expr. Patterns 6, 637–652.

Gerking, S.D., 2014. Feeding ecology of fish. Elsevier.

Hammond, C.L., Moro, E., 2012. Using transgenic reporters to visualize bone and cartilage signaling during development in vivo. Front. Endocrinol. (Lausanne). 3, 91.

Hammond, C.L., Schulte-Merker, S., 2009. Two populations of endochondral osteoblasts with differential sensitivity to Hedgehog signalling. Development 136, 3991–4000.

Hoang, Q.Q., Sicheri, F., Howard, A.J., Yang, D.S.C., 2003. Bone recognition mechanism of porcine osteocalcin from crystal structure. Nature 425, 977–980.

Hosen, M.J., Vanakker, O.M., Willaert, A., Huysseune, A., Coucke, P., De Paepe, A., 2013. Zebrafish models for ectopic mineralization disorders: Practical issues from morpholino design to post-injection observations. Front. Genet. 4, 74.

Huycke, T.R., Eames, B.F., Kimmel, C.B., 2012. Hedgehog-dependent proliferation drives modular growth during morphogenesis of a dermal bone. Development 139, 2371–2380.

Kimmel, C.B., DeLaurier, A., Ullmann, B., Dowd, J., McFadden, M., 2010. Modes of developmental outgrowth and shaping of a craniofacial bone in zebrafish. PLoS One 5, e9475.

Knopf, F., Hammond, C., Chekuru, A., Kurth, T., Hans, S., Weber, C.W., Mahatma, G., Fisher, S., Brand, M., Schulte-Merker, S., Weidinger, G., 2011a. Bone regenerates via dedifferentiation of osteoblasts in the zebrafish fin. Dev. Cell 20, 713–724.

Knopf, F., Hammond, C., Chekuru, A., Kurth, T., Hans, S., Weber, C.W., Mahatma, G., Fisher, S., Brand, M., Schulte-Merker, S., Weidinger, G., 2011b. Bone regenerates via dedifferentiation of osteoblasts in the zebrafish fin. Dev. Cell 20, 713–724.

Laizé, V., Gavaia, P.J., Cancela, M.L., 2014. Fish: a suitable system to model human bone disorders and discover drugs with osteogenic or osteotoxic activities. Drug Discov. Today Dis. Model. 13, 29–37.

Lieschke, G.J., Currie, P.D., 2007. Animal models of human disease: zebrafish swim into view. Nat. Rev. Genet. 8, 353–367.

Liu, H., Cui, J., Feng, W., Lv, S., Du, J., Sun, J., Han, X., Wang, Z., Lu, X., Yimin, Oda, K., Amizuka, N., Li, M., 2015. Local administration of calcitriol positively influences bone remodeling and maturation during restoration of mandibular bone defects in rats. Mater. Sci. Eng. C 49, 14–24.

Luo, S., Yang, Y., Chen, J., Zhong, Z., Huang, H., Zhang, J., Cui, L., 2016. Tanshinol stimulates bone formation and attenuates dexamethasone-induced inhibition of osteogenesis in larval zebrafish. J. Orthop. Transl. 4, 35–45.

MacRae, C.A., Peterson, R.T., 2015. Zebrafish as tools for drug discovery. Nat. Rev. Drug Discov. 14, 721–731.

McClung, M., Harris, S.T., Miller, P.D., Bauer, D.C., Davison, K.S., Dian, L., Hanley, D.A., Kendler, D.L., Yuen, C.K., Lewiecki, E.M., 2013. Bisphosphonate therapy for osteoporosis: benefits, risks, and drug holiday. Am. J. Med. 126, 13–20.

Miller, P.D., 2009. Denosumab: Anti-RANKL Antibody 7, 18–22.

Nakanishi, T., Saito, R., Taniguchi, M., Oda, H., Soma, A., Yasunaga, M., Yamane, M., Sato, K., 2013. In Vivo Determination of Vitamin D Function Using Transgenic Mice Carrying a Human Osteocalcin Luciferase Reporter Gene. Biomed Res. Int. 2013, 895706.

Osathanon, T., Vivatbutsiri, P., Sukarawan, W., Sriarj, W., Pavasant, P., Sooampon, S., 2014. Cobalt chloride supplementation induces stem-cell marker expression and inhibits osteoblastic differentiation in human periodontal ligament cells. Arch. Oral Biol. 60, 29–36.

Patntirapong, S., Habibovic, P., Hauschka, P. V, 2009. Biomaterials Effects of soluble cobalt and cobalt incorporated into calcium phosphate layers on osteoclast differentiation and activation. Biomaterials 30, 548–555.

Pisani, P., Renna, M.D., Conversano, F., Casciaro, E., Muratore, M., Quarta, E., Paola, M. Di, Casciaro, S., 2013. Screening and early diagnosis of osteoporosis through X-ray and ultrasound based techniques. World J. Radiol. 5, 398–410.

Razzaque, M.S., 2011. Osteocalcin: A pivotal mediator or an innocent bystander in

energy metabolism? Nephrol. Dial. Transplant. 26, 42–45.

Singh, S.P., Holdway, J.E., Poss, K.D., 2012. Regeneration of amputated zebrafish fin rays from de novo osteoblasts. Dev. Cell 22, 879–886.

Thomas, G.P., Bourne, A., Eisman, J.A., Gardiner, E.M., 2000. Species-Divergent Regulation of Human and Mouse Osteocalcin Genes by Calciotropic Hormones. Exp. Cell Res. 258, 395–402.

Walker, M.B., Kimmel, C.B., 2007. A two-color acid-free cartilage and bone stain for zebrafish larvae. Biotech. {&} Histochem. Off. Publ. Biol. Stain Comm. 82, 23–28.

Wilkinson, G.F., Pritchard, K., 2014. In Vitro Screening for Drug Repositioning. J. Biomol. Screen. 20, 167–179.

Witten, P.E., 1997. Enzyme histochemical characteristics of osteoblasts and mononucleated osteoclasts in a teleost fish with acellular bone (Oreochromis niloticus , Cichlidae). Cell Tissue Res. 287, 591–599.

Witten, P.E., Hansen, A., Hall, B.K., 2001. Features of mono- and multinucleated bone resorbing cells of the zebrafishDanio rerio and their contribution to skeletal development, remodeling, and growth. J. Morphol. 250, 197–207.

Woeckel, V.J., Alves, R.D.A.M., Swagemakers, S.M.A., Eijken, M., Chiba, H., van der Eerden, B.C.J., van Leeuwen, J.P.T.M., 2010. 1$α$,25-(OH)2D3 acts in the early phase of osteoblast differentiation to enhance mineralization via accelerated production of mature matrix vesicles. J. Cell. Physiol. 225, 593–600.

Yu, P.B., Hong, C.C., Sachidanandan, C., Babitt, J.L., Deng, D.Y., Hoyng, S.A., Lin, H.Y., Bloch, K.D., Peterson, R.T., 2008. Dorsomorphin inhibits BMP signals required for embryogenesis and iron metabolism. Nat. Chem. Biol. 4, 33–41.

Legends

Figure 1. (**A**) Principal bone structures in the cranium of 11-dpf zebrafish after alizarin red S staining. Structures used in the morphometric analysis, i.e. operculum, snout, eye, iris and cleithrum, are outlined in white, while the names of other bony structures are indicated in grey. (**B**) Schematic representation of the head structures assessed through morphometric analysis and parameters measured. *A1*, area of the skull; *A2*, area of the operculum; *L1*, length from the snout to the cleithrum; *L2*, eye width; *L3*, eye height; *L4*, iris width; *L5*, iris height.

Figure 2. Time course of zebrafish operculum development. Fluorescence of the opercula stained with alizarin red S was imaged from 4 to 15 days post-fertilization (**A**) and area of the operculum and head was determined from 10-15 fish for each time point (**B**). Area of the operculum was normalized with the area of the head (*ratio O/H*, **C**). The coefficient of variance (*CV*) is indicated in each graph. Values are presented as the mean ± standard deviation (n≥11). White bar represents 100 μm.

Figure 3. (A-H) Effect of calcitriol exposure (duration and onset) on the osteogenic development of zebrafish operculum (corrected operculum area). **(I)** Diagram recapitulating the different trials (squares) and the parameters of calcitriol exposure (duration and onset of exposure). *Dark grey*, operculum area of control fish exposed to 0.1% ethanol (vehicle); *Light grey*, operculum area of fish exposed to 10 pg/mL of calcitriol. Survival (n) is indicated below each column as n/15, where 15 is the number of zebrafish larvae initially exposed to calcitriol or vehicle. *Asterisks* indicate values statistically different according to Student's *t* test (* $p < 0.05$; *** $p < 0.001$; **** $p < 0.0001$). Values are presented as the mean ± standard deviation.

Figure 4. Pro/anti-osteogenic effects of calcitriol and cobalt chloride on zebrafish operculum. Changes in operculum area are expressed as percentages over the respective control (0.1% ethanol for calcitriol and water for cobalt chloride). Survival (n) is indicated in each column as n/15, where 15 is the number of zebrafish larvae initially exposed to each compound. *Asterisks* indicate values statistically different from vehicle values (one-way ANOVA followed by Dunnett's multiple comparison

test (* $p < 0.05$; **** $p < 0.0001$). Values are presented as the mean ± standard deviation.

Figure 5. Effects of calcitriol and cobalt chloride exposure (from 3 to 6 dpf) on the expression of *osterix* and *osteocalcin* in the operculum of double-transgenic zebrafish larvae *Tg(sp7:mCherry/oc:EGFP).* (**A**) Morphometric analysis of the fluorescence signals in the operculum of calcitriol-treated larvae (6 dpf) of the double-transgenic zebrafish line. Red (*sp7:mCherry*) and green (*oc:EGFP*) channels were merged and the following parameters were determined using built-in tools in ImageJ: *Left panel*, total area of red (red dashed-area) and green (green dotted-area) fluorescence, and *right panel,* number of red and green pixels above threshold values in the operculum (white dashed-area). (**B**) Fluorescence images of the operculum from controls (0.1% ethanol, EtOH; water, H_2O), calcitriol (10 pg/mL) and cobalt chloride (4 mg/L) treated larvae. (**C**) Corrected red and green opercular area (percentage over the control). (**D**) Number of red and green pixels per operculum area. *Asterisks* indicate values statistically different according to Student's *t* test (* $p < 0.05$; ** $p < 0.01$; **** $p < 0.0001$). Values are presented as the mean ± standard error of the mean ($n \geq 15$). Scale bars in A and B represent 50 μm.

Figure 6. Flowchart showing the steps of the screening process using the zebrafish operculum system. * temperature 28 ± 0.1 °C, pH 7.5 ± 0.1, conductivity 700 ± 50 μS, NH_3 and NO_2 lower than 0.5 mg/L, NO_3 at 5 mg/L. ** Time depend on operator skills.

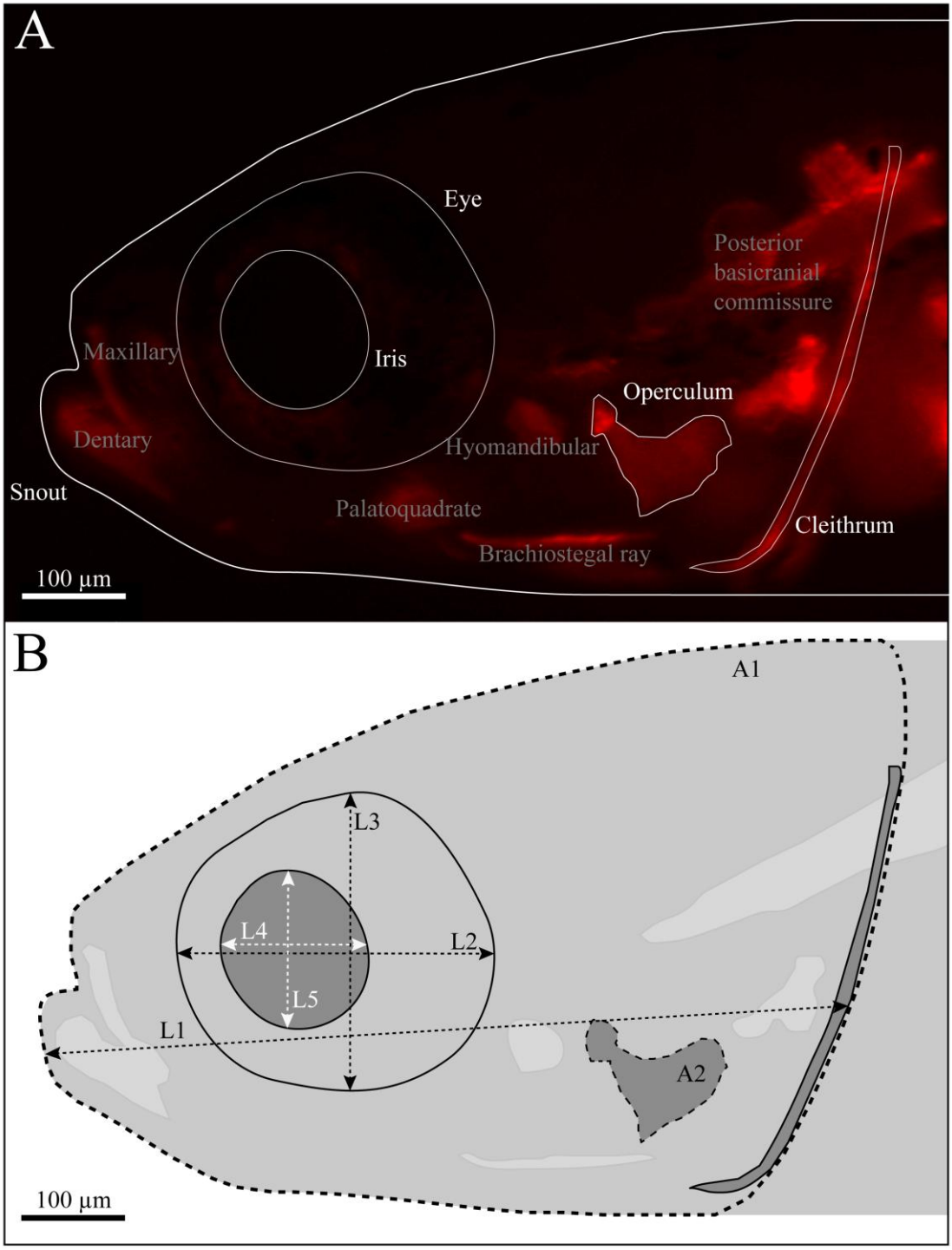

Figure 1

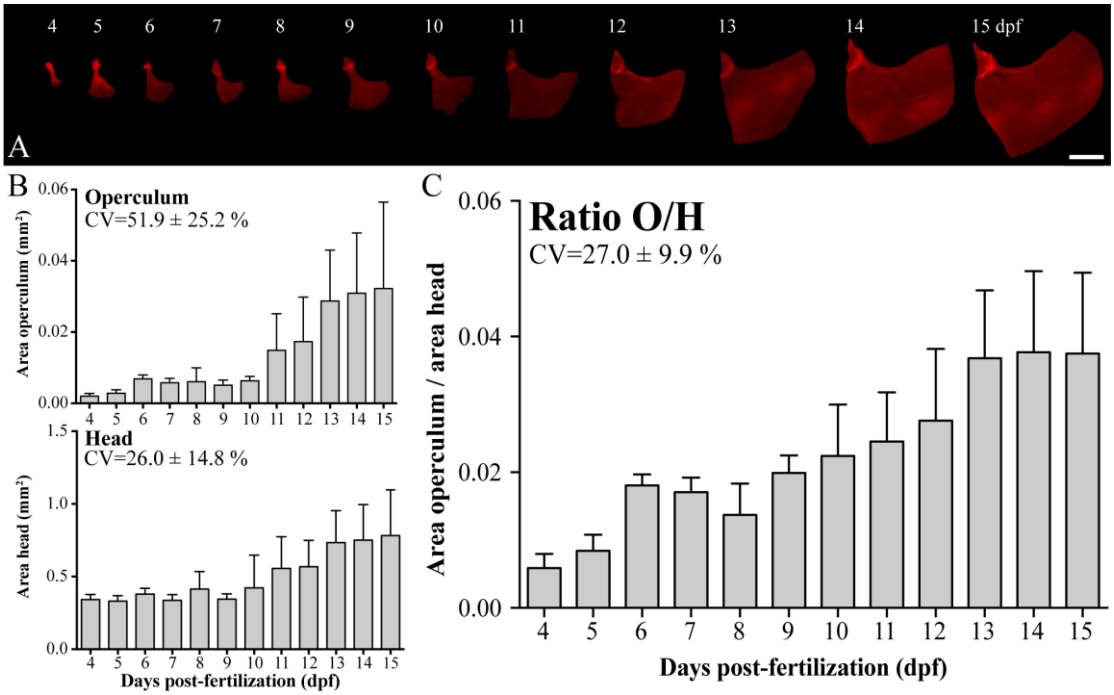

Figure 2

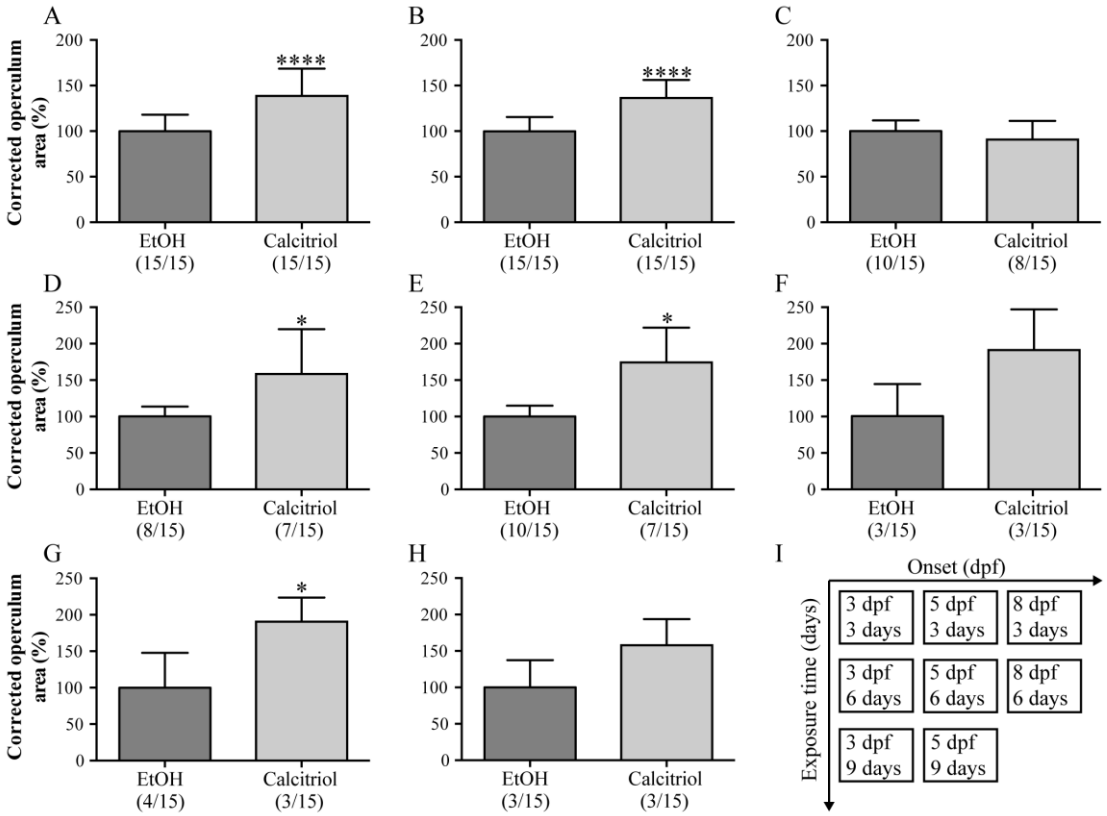

Figure 3

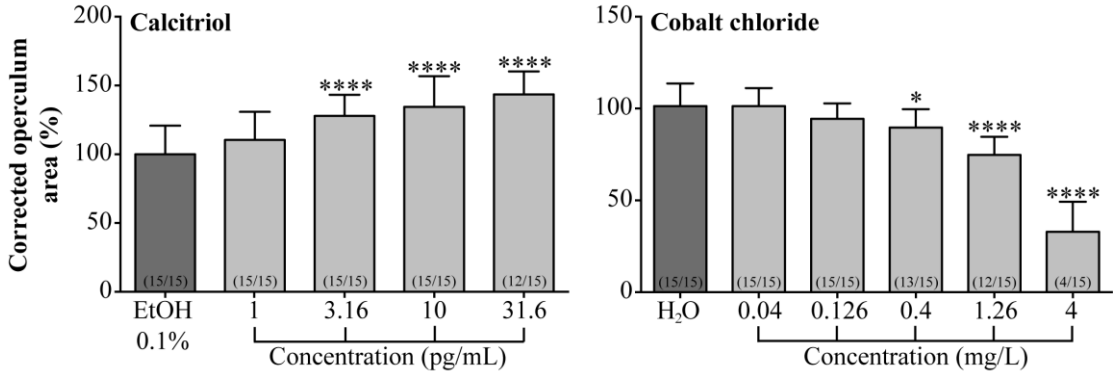

Figure 4

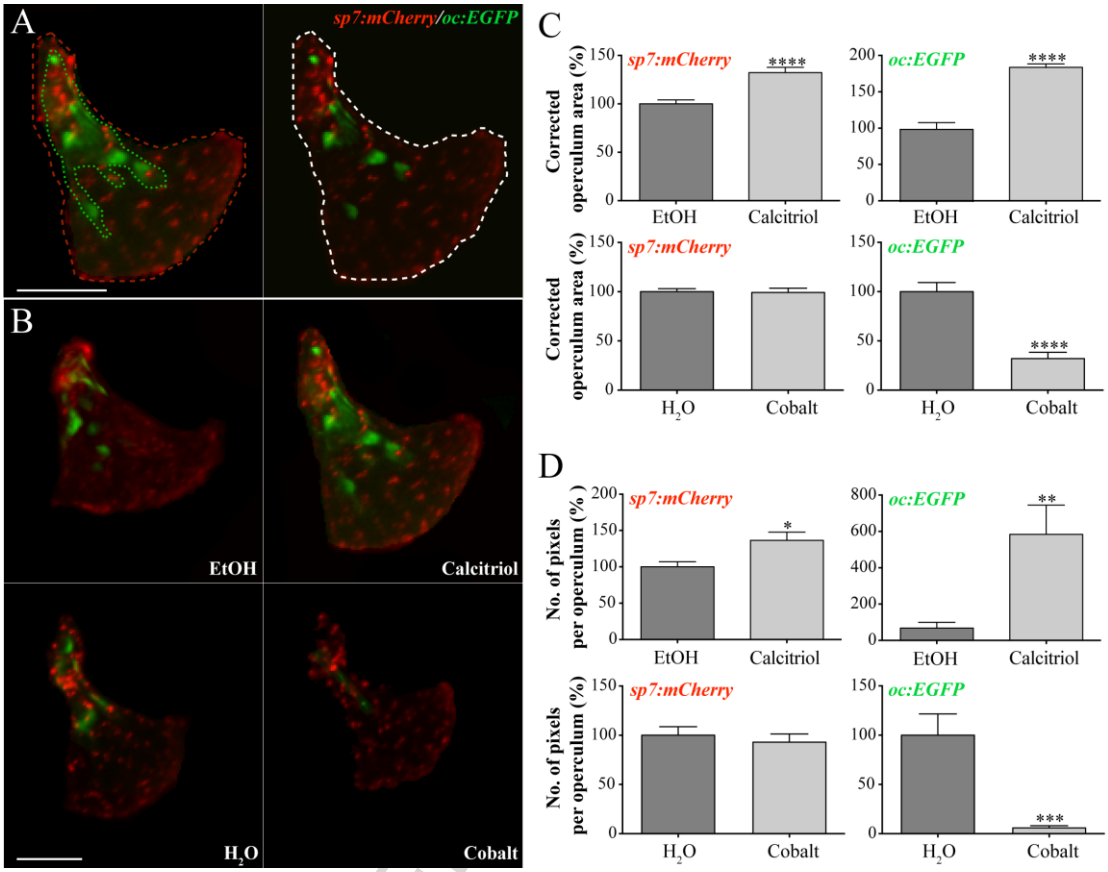

Figure 5

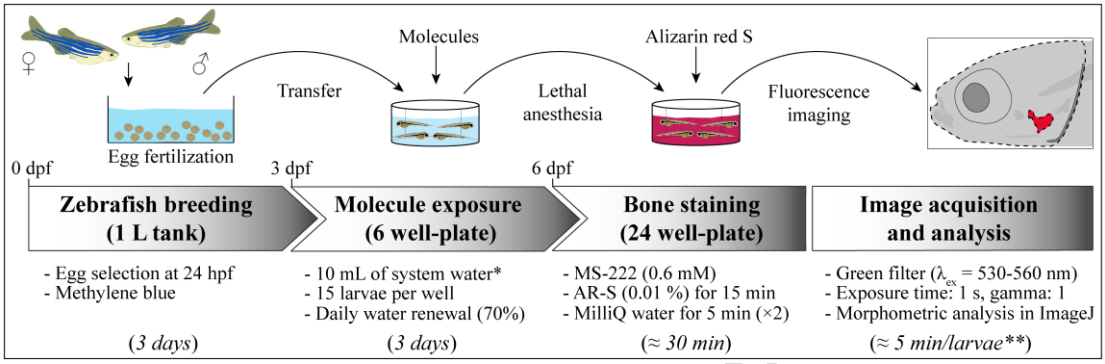

Figure 6